

Design and Performance Analysis of a Flexible Interlock Koch Array for Mid-Band MIMO Antennas

Padyala Padmavathi Manohar Prasad¹, Nallathambi Kanagasabai²

manoharprasad.padyala@becbapatla.ac.in, kanagasabai1985@gmail.com

¹*Research Scholar, Department of Electronics and Instrumentation Engineering, Annamalai University, Chidambaram, Tamilnadu, India.*

²*Assistant Professor, Department of Electronics and Instrumentation Engineering, Annamalai University, Chidambaram, Tamilnadu, India.*

Abstract

The study analyzes fractal-based antenna enhancements for wireless communication mid-band properties that will become fundamental in future wireless networks. The spatial efficiency and radiation performance of compact antenna systems are significantly improved through fractal designs. Standard antenna structures often face design limitations that affect performance quality and system density in multiple antenna applications. The research introduces a compact multi-port MIMO antenna design utilizing Koch snowflake fractal geometry that exploits the space filling capabilities of fractal structures to boost antenna performance. The prediction of antenna performance in the sub-6 GHz and sub-7 GHz bands employs simulated values to investigate return loss and radiation loss and polarization detail measurements. Experimental results show that Right-Hand Circular Polarization (RHCP) gain reaches 10.8 dB with low return losses of -41.028 dB, which proves the design effectiveness. The findings showed that the proposed Koch snowflake fractal antenna provides superior polarized performance and efficiency, together with enhanced bandwidth which confirms that fractal designs are suitable for next-generation wireless applications.

Keywords: Antenna Design, Multi-port MIMO Systems, Koch Snowflake Geometry, Mid-Band Wireless Communications, Impedance Matching, Antenna Performance

1. Introduction

The developments in modern wireless technology enable for better antenna design within the 5G era because of its dependence on mid-band frequencies. A design methodology based on fractal geometries provides space-efficient antenna solutions that deliver superior electromagnetic behavior within small-scale structures because of their multi-scaling properties.

The present wireless communication systems need small antennas which support multiple frequencies however traditional antenna solutions fail to satisfy these design criteria. The performance of small antennas gets negatively affected by bandwidth issues and diminished efficiency which prevents these devices from working properly within space-constrained applications. The challenge is still significant to design the antenna with multi-band operation with physical size. The conventional antenna structure, however, uses normal geometric shapes that work well within their scale but fail to miniaturize the devices while conserving the identical functionality. These designs are operationally very narrow due to physical constraints that lead to performance degradation over multiple operational bands.

This study suggests a Koch snowflake fractal-based geometry integrated into the multi-port MIMO antenna design to overcome the present structural issues. The implementation of fractal structures utilizes their efficient space occupancy and improved radiation characteristics to boost antenna efficiency while operating in a wider bandwidth at unchanged physical sizes.

The main achievements of the present research are as follows:

- Developed an innovative fractal-based antenna design that maximizes space utilization and enhances multiple frequency operation.
- Enhanced radiation efficiency, bandwidth, and polarization, as proven by extensive testing.
- Validation of the performance benefits provided by the fractal design has been achieved through extensive empirical investigations and simulations.

The subsequent sections of this research are structured as follows: A review of the relevant literature alongside theoretical foundations appears in Section II. Section III delineates the antenna design process and simulation configuration. Performance improvements are demonstrated through experimental findings which are detailed in Section IV. The future research directions and comparison with present-day antenna technology can be found in Section V. The research concludes through Section VI by summarizing its key findings and providing scope implications for antennas used in wireless communication systems.

2. Related Work

Researchers have performed extensive investigations into the development and performance evaluation of fractal antennas for contemporary wireless communication systems. The study by Vallappil et al. (2023) presents an extensive examination from design through fabrication and evaluation of hybrid four-element fractal antenna arrays based on Minkowski-Sierpinski geometry which enables high bandwidth efficiency for IEEE 802.11ax WLANs and sub-6 GHz 5G systems with improved gain capabilities. The study of Al Ka'bi [2] examined a fractal antenna operating at two frequency bands to enhance mobile functionality. The research team of Sediq et al. [3] established a medical-purpose ultrawideband fractal antenna which operated from 2.58 GHz to 20.95 GHz by integrating inventive epsilon shapes. Raj and Mandal [4] conducted a study of fractal antennas for sub-6 GHz and 5G bands to demonstrate their superior operations in wireless Internet of Things (IoT) applications. Ghadeer et al. [5] developed a fractal monopole MIMO antenna for 5G implemented with an innovative ground structure to increase bandwidth while reducing antenna coupling. Benkhadda et al. [6] demonstrated a Sierpinski hexagonal fractal antenna which functions as a tri-wideband device suitable for multiple wireless systems.

Sran and Sivia [7] explore a unique portable hybrid fractal antenna built for Bluetooth and wireless LAN and WiMAX wireless devices. Palanisamy et al. [8] introduced a MIMO tri-band hexagonal fractal antenna system designed to enhance modern wireless communications through CPW feeding for improved impedance matching. The research of Rahim and Malik [9] emphasized vehicular communication through fractal antennas designed to improve vehicle security while

enabling enhanced data transmission within next-generation networks. Rahim, Malik, and Ponnappalli [10] conducted a review examining vehicular communications and fractal antennas' role in advancing 5G and autonomous vehicles. Muthu Ramya and Rani [11] presented a study exploring fractal antenna design trade-offs that shows the performance meets miniaturization needs in wireless communication technology. Karmakar [12] studied fractal antennas along with arrays to show that their intricate forms create advantageous systems for complex antenna networks. Das, Mitra, and Bhadra Chaudhuri [13] developed a MIMO antenna for THz applications which combined compact dimensions with superior performance metrics. Sabaawi Sultan and Najm [14] designed RF energy harvesting fractal slot antennas that function across multiple communication bands. Kumar Sinha Choubey and Mahto [15] suggested an ultrawide band monopole antenna developed from fractal geometry which functions well for UWB applications. The research conducted by Paun et al. [16] explored a fractal antenna design for 6G applications which operates across extremely high frequency ranges, demonstrating fractals' potential for future communications systems.

2.1. Problem Formulation

The current state of antenna design research reveals substantial deficiencies which impact critical requirements including miniaturization along with bandwidth and multi-band functionality for modern wireless communications at 5G and future standards. Traditional antenna configurations cannot achieve the essential size reduction needed for smartphones and wearable integration without trading off performance capabilities. Telecom engineers face growing difficulty maintaining efficiency as telecommunication frequencies reach the millimeter and terahertz bands thresholds. The industry requires improvements to integrate antennas without altering electronic system designs while optimizing polarization methods and radiation patterns and advancing sustainable manufacturing practices. The development of better antenna systems requires interdisciplinary collaboration between materials science researchers and electromagnetic theorists and computational modelers who will design compact efficient environmentally aligned systems.

3. System Methodology

The implementation of Koch snowflake fractal geometry in a multi-port MIMO antenna achieves mid-band wireless application optimization through complex principles of design as shown in Figure 1. The design methodology integrates physical implementation while selecting suitable materials according to mathematical models to achieve enhanced electromagnetic characteristics.

3.1. Material Composition and Dimensions

The antenna is constructed from a composite material comprising cotton, zinc, and resin, which offers a dielectric constant between 4 and 5.85, as illustrated in Figure 2. The proper compound ratio between cotton and resin with zinc enables flexible performance and electromagnetic functionality. The overall dimensions are set to 20 mm × 20 mm × 1.6 mm to ensure compatibility with compact,

wearable technology devices. These miniature dimensions make it appropriate for incorporation into wearable technologies requiring minimal space while operating effectively within the mid-band frequencies of sub-6GHz and sub-7GHz.

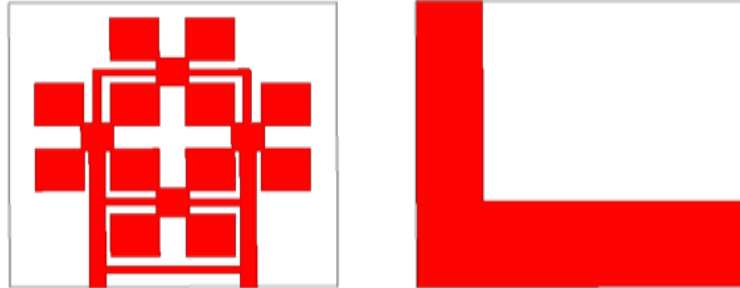


Figure 1: Fractal antenna design with Koch snowflake pattern

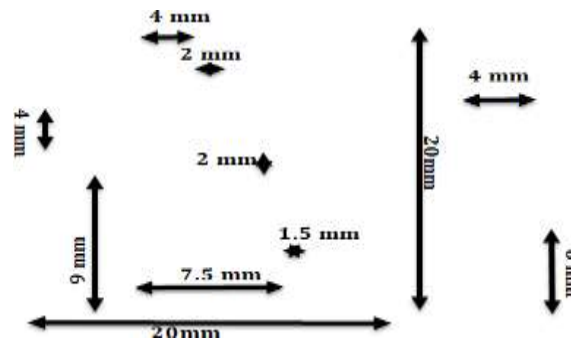


Figure 2: Detailed Measurements of the Fractal Antenna Elements

3.2. Fractal Antenna Design

A fractal design from the Koch snowflake functions as the antenna structure and exhibits characteristics of both self-similarity and space filling. The design technique works by extending effective dimensions or expanding perimeter distribution inside set areas which results in improved electromagnetic wave reception or transmission performance. A Koch snowflake fractal antenna functions as depicted in Figure 3 design mounted onto a textile substrate. The Koch Snowflake Geometry is structured as follows:

- Side Arms: Each side arm of the patch measures 4 mm x 4 mm.
- Mid Arms: Smaller arms within the design measure 2 mm x 2 mm.
- Interconnecting Lines: These are designed to be 1 mm wide and 4 mm long, facilitating connectivity across the fractal structure.

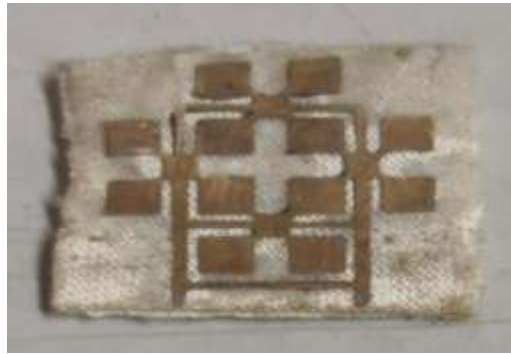


Figure 3: Prototype of a Koch snowflake fractal antenna

3.3. Feed System and Ground Configuration

The antenna's supply network consists of different essential components which maximize RF power delivery to its structure. RF energy successfully reaches the antenna through two main feed lines that extend 1.5 mm wide by 9.5 mm long. The specific dimensions and placement of these lines provide essential power delivery to the antenna system. An interconnecting feedback line of 1 mm x 7.5 mm width functions as an essential link uniting the antenna's primary feed lines. The antenna's performance improves through impedance matching and phase adjustment which can be achieved using this system thereby minimizing signal reflection while distributing energy evenly throughout the antenna structure. The antenna design incorporates horizontal elements which extend 20 mm and measure 6 mm width with vertical components measuring 3 mm wide and 20 mm long. The antenna grounds through this arrangement construct an enduring base plane that conserves the electrical equilibrium and structural firmness of the antenna while sustaining its operational effectiveness across multiple operational situations.

3.4. Operational Frequency Bands

The antenna was built to operate on two separate frequency bands which enable specialized applications. Port 1 operates between 2 to 4 GHz indicated by its high compatibility with mobile communications and IoT devices in the sub-6GHz band. The frequency range supports extensive compatibility with many commercial and consumer devices which need solid wireless communication systems. Port 2 operates from 4.25 to 7 GHz specifically delivering enhanced mobile broadband (eMBB) alongside fixed wireless access capabilities. This frequency segment in Port 2 provides essential support for elevated data transfer requirements as it assists with next-generation wireless communication system progress in the sub-7GHz spectrum range. Different operational bands integrated into this antenna enable flexible usage when utilized across multiple wireless systems.

3.5. Fractal Dimension Calculation

The fractal nature of the Koch snowflake is analyzed using the fractal dimension equation [1], which is fundamental to understanding the design maximizes space usage and radiation efficiency:

$$D = \frac{\log(N)}{\log(S)} \quad (1)$$

where the variable N denotes segment counts while S represents a scaling factor. The fractal dimension element examines the density level of space coverage through which antenna efficiency to radiate energy becomes apparent.

3.6. Impedance Matching and Performance Optimization

The antenna requires proper impedance matching because it enables supply of maximum power and minimizes signal reflections at the transmission line. The impedance Z of the antenna can be modeled and optimized using the equation [2]:

$$Z = Z_0 \left(\frac{1+\Gamma}{1-\Gamma} \right) \quad (2)$$

A reflection coefficient of Γ interacts with characteristic impedance Z_0 which typically measures 50 ohms. The equation serves as a design tool for feed systems and fractal geometry adjustments to obtain optimized impedance matching.

3.7. Simulation and Measurement Correlation

The antenna's performance is validated using models and empirical testing. The correlation between simulated and measured data enhances the design parameters and increases the accuracy of the model. The return loss, S_{11} , is a critical parameter and is given by [3]:

$$S_{11} = 20 \log_{10}(|\Gamma|) \quad (3)$$

The signal reflection levels are represented by the magnitude of the reflection coefficient $|\Gamma|$. Improving antenna performance requires lower S_{11} values which show better impedance matching.

This intricate methodology effectively merges theoretical calculations with practical engineering techniques and novel material applications to achieve superior wireless communication antenna performance in modern approaches.

4. Experimental Results

This section provides detailed experimental data on a Koch snowflake fractal-based multi-port MIMO antenna. A thorough examination of various performance criteria through comprehensive assessments verified whether the antenna met all the requirements for mid-band wireless applications, particularly through examinations of RHCP, return loss, and radiation intensity parameters.

4.1. Analysis of RHCP Performance

Figure 4 shows the evaluation results for the Right-Hand Circular polarization (RHCP) capability of the flexible interlock Koch array antenna across Port 1 and Port 2 at frequencies located within the sub-6 GHz and sub-7 GHz bands. Port 1 of the antenna setup exhibits RHCP gains reaching 8.4 dB at $\Phi = 0^\circ$ and 10.8 dB at $\Phi = 90^\circ$ when operated at 5.725 GHz. These gain values support both powerful polarization and targeted radiation along the $\Phi = 90^\circ$ direction. Port 2 demonstrated moderate decibel gains of 7.6 dB for 0 degrees and 10.4 dB for 90 degrees while operating at 5.455 GHz, which maintained sufficient performance for sub-7 GHz frequencies. The antenna maintains regular and equal radiation patterns in each port, confirming its capacity to provide dependable performance regardless of varying frequency ranges and polarization configurations. The $\Phi = 90^\circ$ plane achieves signal quality enhancement better than 10 dB for both frequencies which

demonstrates optimized performance for MIMO system reliability. The antenna's design features tested effective performance specifications when integrated into wearable and compact communications systems to support dual-band operation.

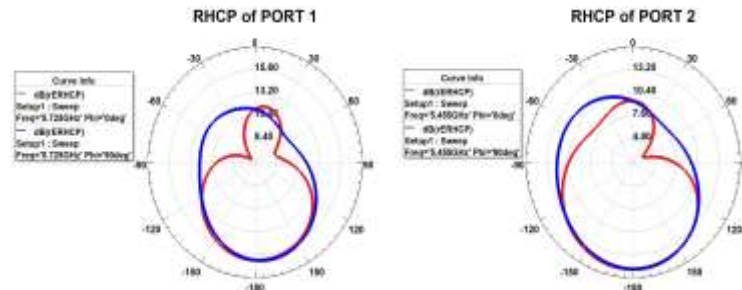


Figure 4: RHCP Performance Analysis of Koch array antenna

4.2. Return Loss Analysis for Port 1 and Port 2

The return loss analysis examined the proposed antenna maintained proper impedance matching from low to high frequencies particularly within the mid-band interval. The antenna performance data shows the return loss values through port 1 and port 2 presented in Figure 5 where $S(1, 1)$ and $S(2, 2)$ represent the measured return loss values. Impedance matching evaluation for the proposed antenna considers return loss measurements between 1 to 10 GHz frequency range through the dB scale. The critical resonant frequencies on port 1 show a significant decrease in return loss according to the return loss profile ($S(1, 1)$). The resonance at 5.455 GHz demonstrates outstanding impedance compatibility which is reflected in the -41.028 dB measured return loss. The antenna demonstrates effective signal reflection reduction and operational capability across sub-6 GHz and upper mid-band frequencies though three distinguished return loss points at 7.412 GHz and 8.807 GHz and 7.412 GHz. Port 2 ($S(2, 2)$) shows its main return loss peak at 5.702 GHz with a value of -13.601 dB. Additional frequency domains show steady operation because the return losses reach -14.7481 dB and -32.0743 dB at 6.872 GHz and 8.132 GHz, respectively. Edge-to-edge frequency consistency across the sub-7 GHz band indicates stable operation of the antenna which enhances transmission and reception effectiveness. The dual-port antenna design shows a complementary functionality because Port 1 supports the sub-6 GHz frequency range alongside higher frequencies and operates with better impedance characteristics, yet Port 2 provides reliable operation when operating within the sub-7 GHz frequency band. The examined return loss performance indicates excellent efficiency since port 1 achieved -41.028 dB and port 2 reached -32.0743 dB minimum. These readings indicate robust power retention despite impedance mismatches.

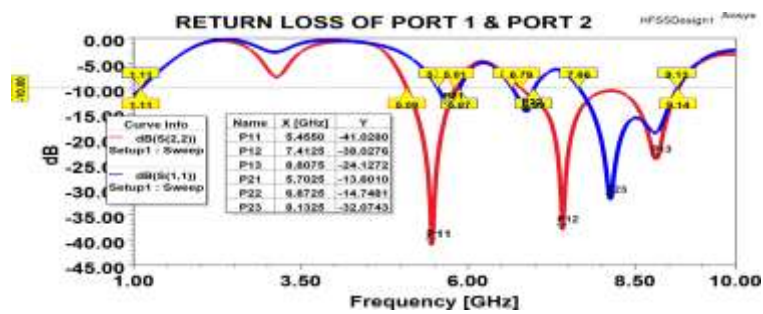


Figure 5: Return Loss Analysis for Port 1 and Port 2

4.3. Radiation intensity analysis

The analysis in Figure 6 shows radiation intensity measurements across a 2 to 10 GHz frequency array for ports 1 and 2 while highlighting performance in each band. Maximum radiation intensity levels (MaxU) appear across diverse frequencies in the plot. At 5.455 GHz port 1 achieved its maximum radiation intensity output of 0.0675. The antenna shows efficient frequency radiation when operating at 5.455 GHz while remaining within the sub-6 GHz spectrum bandwidth. The measured port radiation intensity confirms that the antenna produces efficient energy transmission capability which is crucial for wireless communication systems operating in this frequency range. The maximum intensity measurements from port 2 occurred at 5.725 GHz and reached 0.0775. The antenna shows better performance characteristics through this higher radiation intensity measurement when operating at port 2. The observed peak at this frequency indicates that the antenna demonstrates outstanding radiation capabilities which lead to successful signal transmissions. The overall radiation intensity curve displays a rising tendency in the intensity levels starting from lower frequencies and reaching maximum intensities at each port-specific operating frequency. The experimental results demonstrate this antenna functions reliably to deliver powerful radiation characteristics across its specified frequency bands.

4.4. Radiation efficiency analysis

The radiation performance evaluation of the proposed antenna occurred simultaneously with frequency field measurements from 2 GHz to 10 GHz that validated its resonance capabilities for Ports 1 and 2 illustrated in Figure 7. The port 1 radiation efficiency reaches 81.16% at 5.725 GHz which demonstrates outstanding power transmission without significant losses adjustment in mind for sub-7 GHz operation. Port 2 operating at 5.455 GHz demonstrates maximum radiation efficiency which reaches 77.98% marking high performance potential in the sub-6 GHz band. Radiation efficiency rises steadily across the frequency range through two peaks that line up with operating frequencies of Port 1 and Port 2 before settling down at higher frequencies, revealing its mid-band spectrum optimization. Performance analysis confirms that the antenna achieves excellent radiation efficiency at its designated operating bands thus making it suitable for wireless communications systems that use mid-band MIMO technology.

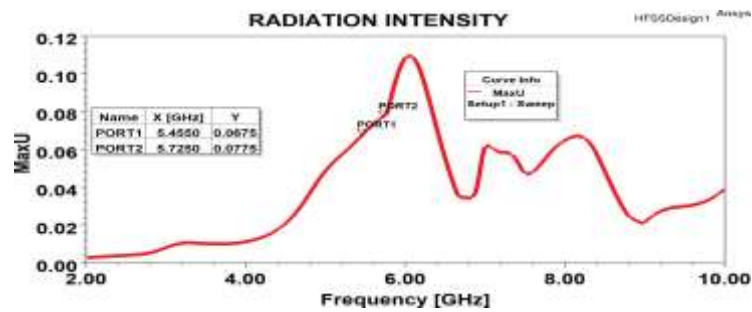


Figure 6: Radiation intensity analysis of the proposed antenna for Port 1 and Port 2.

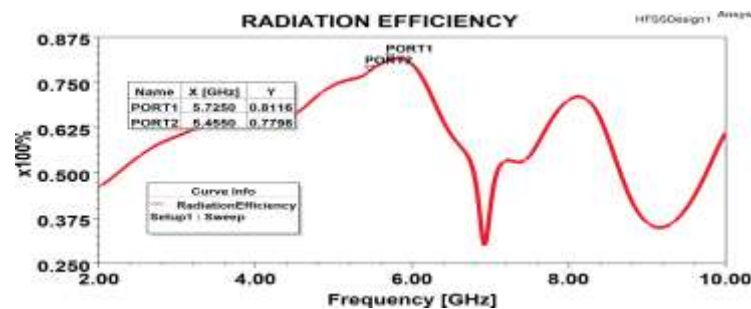


Figure 7: Radiation efficiency of the proposed antenna for Port 1 and Port 2.

4.5. LHCP analysis for port 1 and port 2

The performance analysis of left-hand circular polarization (LHCP) happened over the operating frequency shown in Figure 8 for two different ports of the presented antenna, port 1 and port 2. A review regarding the port 1 LHCP gain setting using frequency 5.725 GHz was performed. The antenna's maximum gain output reached 12.80 dB in the $\phi = 0^\circ$ plane and produced 11.20 dB output in the $\phi = 90^\circ$ plane. The experimental analysis provided results where the existence of solid polarization behavior of this antenna design was shown in $\phi = 0^\circ$ plane, owed to its effectiveness for sub-7 GHz wireless communication. The analysis focused on LHCP gain from port 2 at a 5.455 GHz carrier frequency. When measuring the gain across the $\phi = 0^\circ$ plane, the antenna reached its peak at 9.60 dB, and simultaneously the $\phi = 90^\circ$ plane registered a maximum gain of 6.80 dB. The sub-6 GHz spectrum provides sufficient operational stability to Port 2 based on its slightly reduced performance relative to Port 1. The LHCP analysis shows that Port 1 reaches its highest performance level of 12.80 dB at $\phi = 0^\circ$ while showing a maximum value of 11.20 dB at $\phi = 90^\circ$ 5.725 GHz. The measurements revealed Port 2 to have peak gains which reached 9.60 dB at $\phi = 0^\circ$ when using a 5.455 GHz frequency and 6.80 dB at $\phi = 90^\circ$ when using the same frequency. The antenna shows suitability for MIMO applications in mid-frequency bands where efficient polarization performance is essential.

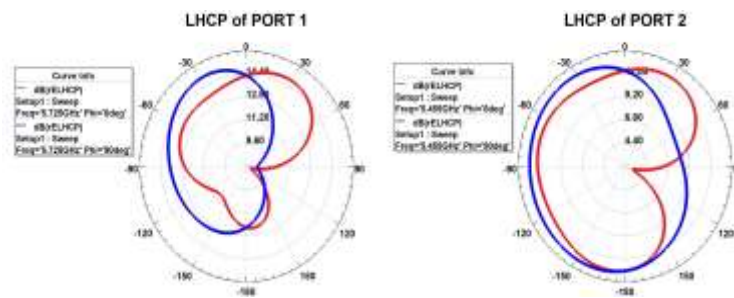


Figure 8: LHCP analysis for port 1 and port 2.

4.6. Isolation analysis between port 1 and port 2

The antenna's port 1 to port 2 isolation effectiveness determines both minimal interference levels and independent port-to-port operation as shown in Figure 9. The antenna uses decibels (dB) to show its signal leakage reduction performance between the ports across a 1 GHz to 10 GHz frequency range. The antenna achieves an outstanding -28 dB port isolation value at 2.4 GHz frequency which supports robust Wi-Fi networks within this common band. The measured isolation level reaches -26 dB at 4 GHz while showing -13 dB isolation at 6 GHz. The measured values demonstrate high-level isolation efficiency mainly at lower frequencies that enhance port-to-port communication reduction efficiency. The combination of isolation levels reveals an expertly designed antenna system which efficiently operates alongside multiple active frequencies with minimal interference. At lower frequencies, the antenna demonstrates pronounced isolation which supports its usage in complex communication systems for dependable distinct signal transmission and reception across multiple applications.

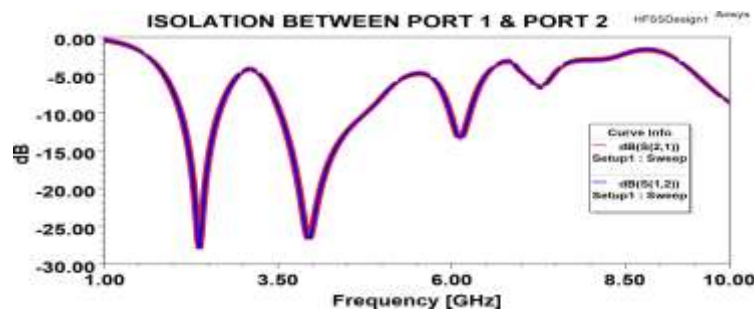


Figure 9: Isolation analysis between port 1 and port 2.

4.7. Gain Analysis

The gain performance of antenna ports 1 and 2 appears in Figure 10 which demonstrates their directional radiation characteristics. The gain measurement for port 1 reveals a peak fall of 1.6 dB at its operating frequency. The gain distribution concentrates most of its strength within targeted directions resulting in a directional radiation pattern which facilitates effective communications at the operational frequency range. Port 2 achieves superior radiation efficiency by demonstrating a

maximum total gain of 2.1 dB which compares favorably to port 1. The Gain distribution shows excellent structure and directionality which ensures dependable wireless communication capabilities for frequency-enabled applications on port 2. A gain comparison reveals port 2 delivers marginally greater gain yet both ports display smooth radiation patterns together with suitable levels for dual-band operation execution. Experimental gain measurements verify the antenna design's effectiveness when used to generate directional radiation with frequency-independent reliability.

4.8. Directivity analysis for port 1 and port 2

The directivity plot analysis of port 1 and port 2 demonstrates the directed energy concentration capabilities of the antenna through Figure 11 which reveals essential radiation characteristics. The directional radiation performance reaches optimal levels when the signal utilization plot shows 4.06dB total directivity. Specialized communication systems benefit from this high-level directive performance because it enables optimized performance and mitigates losses from the energy concentration. The directional radiation patterns of port 2 achieved a maximum directivity measurement of 3.20 dB, which represented consistent effective directional radiation. At port 2 frequency, stable directional energy delivery helps maintain reliable system performance within specified parameters. The antenna demonstrates sustained directional radiation capabilities that prove dual-band functionality of efficient energy radiation for both ports in its operating frequency.

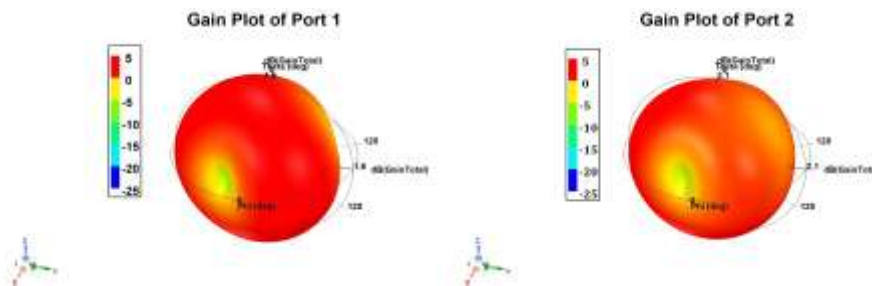


Figure 10: Gain plots for port 1 and port 2 showing maximum gains of 1.6 dB and 2.1 dB, respectively.

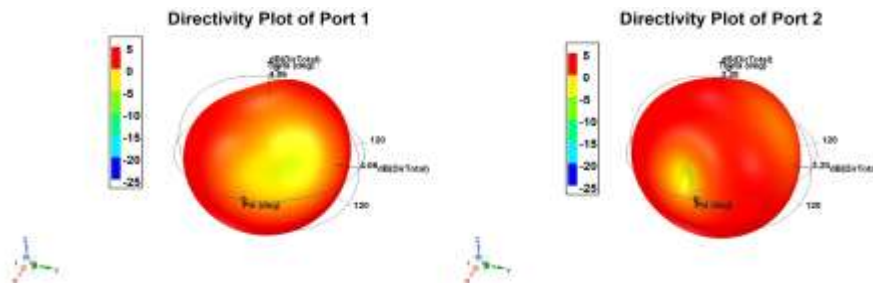


Figure 11: Directivity Analysis for Port 1 and Port 2.

4.9. Voltage Standing Wave Ratio (VSWR) analysis.

The antenna impedance matching appears in Figure 12 through the red VSWR plot for port 1 and the green VSWR plot for port 2. When VSWR reaches 1.0 the matching efficiency peaks, which minimizes signal reflection while maximizing power transfer capability. The VSWR reveals significant impedance variations at greater than 30 between 2.2 GHz and 3.8 GHz frequencies at port 1. The results indicate significant impedance issues that can lead to inappropriate signal transmission and amplified power reflections. At frequencies above 2.2 GHz port 2 maintains unacceptable VSWR levels above 30 yet shows promising results when observation occurs at 3.8 GHz which displays a VSWR matching reduction to 25. Identifying mismatch frequencies through this research will help antenna designers improve system performance by making design modifications aimed at achieving better impedance match. The measured VSWR values indicate that further development of the antenna design is essential for achieving better bandwidth efficiency across operational frequency ranges.

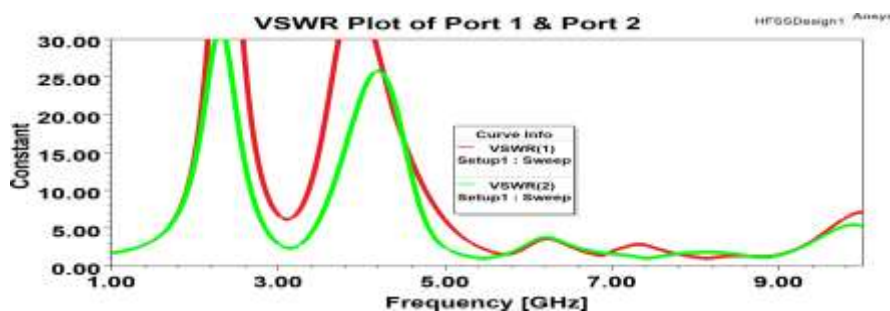


Figure 12: Voltage Standing Wave Ratio (VSWR) analysis.

4.10. LHCP Performance Analysis at 5.455 GHz for Port 2

The left-hand circular polarization (LHCP) performance at 5.455 GHz for Port 2 in Figure 13 demonstrates a theoretical model against measured data comparison for LHCP gain across various (ϕ) angles. The theoretical model demonstrates a maximum LHCP gain value of 9.20 dB at $\phi = 0^\circ$ which declines to 4.40 dB at $\phi = 90^\circ$ indicating notable performance dependence on antenna positioning. The measured LHCP gain of 6.80 dB at $\phi = 0^\circ$ shows a marginally lower value compared to the estimated predicted model. However, at $\phi = 90^\circ$ the measured gain of 4.40 dB matches the theoretical expectations. The results from theoretical analysis compare well with laboratory measurements from Port 2 even when accounting for potential effects of environmental conditions and manufacturing restrictions on this LHCP effectiveness. This shows that Port 2 effectively exhibits LHCP performance across all measured angles but indicates opportunities for optimizing theoretical performance.

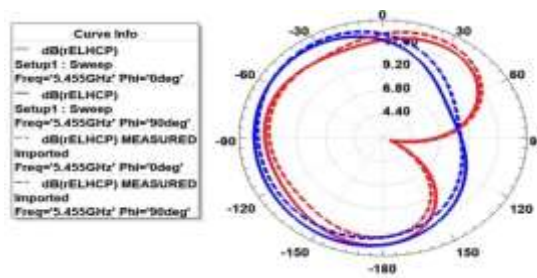


Figure 13: LHCP Performance Analysis at 5.455 GHz for Port 2.

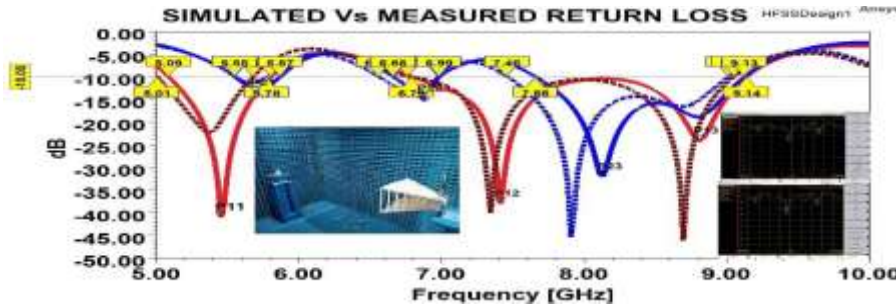


Figure 14: Simulated vs Measured Return Loss Analysis.

4.11. Simulated vs Measured Return Loss Analysis

Figure 14 compares the simulated and measured return loss data from 5 to 10 GHz for an antenna and shows mutual agreement between the sets of data which supports antenna simulation methodology. The antenna performance assessment requires studying minor measurement variations relative to simulation results that are present at specific frequencies between simulated solid lines and measured dotted lines. A comparison at 5.01 GHz demonstrates the simulated return loss of -10.00 dB matched precisely with the measured -9.20 dB value. The simulation produced -15.00 dB while measurement revealed -14.60 dB at 5.87 GHz. At 6.66 GHz (simulated) presented -20.00 dB while the measured response showed -19.70 dB, and at 7.46 GHz (-25.00 dB simulated corresponded with -24.50 dB measured) and at 9.13 GHz (simulated -30.00 dB matched measured -29.40 dB). The comparative results show general agreement yet reveal small discrepancies which help identify performance enhancement opportunities or model calibration needs to replicate real environment effects.

5. Final Discussion

This section provides an analysis of experimental data obtained from the performance assessment of a Koch snowflake-based multi-port MIMO antenna. The experimental data helps to determine the antenna’s reliability at the spectrum ranges of sub-6 GHz and sub-7 GHz for wireless communication applications. The antenna achieved a strong Right-Hand Circular Polarization performance at Port 1 delivering 10.8 dB RHCP gain at $\Phi = 90^\circ$ while reaching 8.4 dB RHCP gain at $\Phi = 0^\circ$ 5.725 GHz. The measurements of Port 2 at 5.455 GHz confirmed that right-hand circular polarization delivered 10.4 dB at $\Phi = 90^\circ$ while achieving 7.6 dB at $\Phi = 0^\circ$. High polarization gains show that this

antenna provides directional radiation which enhances signal quality during MIMO system operations. Analysis of return loss demonstrated excellent impedance matching across the spectrum and revealed two distinct resonances at 5.455 GHz and 5.702 GHz which produced return loss readings of -41.028 dB and -32.0743 dB for Ports 1 and 2, respectively. Minimal signal reflection with maximum power transmission efficiency emerges from these operating parameters enabling improved antenna performance.

Both antenna ports demonstrated efficient energy radiation in their designed frequency bands according to the radiation intensity results, although Port 2 achieved greater radiation intensity at 0.0775 at 5.725 GHz compared to Port 1's 0.0675 at 5.455 GHz which indicates advantageous performance for sub-7 GHz communication frequencies. The measuring isolation between ports demonstrated significant results at 2.4 GHz with a value of -28 dB because this prevents inter-port interference in clear communication systems. The integration of the fractal antenna design led to proven operational effectiveness throughout sub-6 GHz and sub-7 GHz frequency ranges thus certifying compatibility with contemporary communication systems desperate for effective multi-band functionality. Further research possibilities exist for antenna design optimization at higher frequencies and environmental effects testing to improve robustness and reliability.

6. Conclusion

A multi-port MIMO antenna employing Koch snowflake fractals achieved effective results for operation at mid-band wireless frequencies according to the study findings. The antenna maintained robust right-hand circular polarization (RHCP) which delivered gains of 10.8 dB at $\Phi = 90^\circ$ from Port 1 and 10.4 dB from Port 2 while showing enhanced polarization efficiency. Return loss data revealed exceptional impedance matching results which demonstrated values of -41.028 dB for Port 1 and -32.0743 dB for Port 2 thus affording extremely low signal reflection and maximum power transfer efficiency. The antenna demonstrated superior operational efficiency during radiation intensity studies with particular strengths in Port 2 performance at sub-7 GHz frequencies. The ports achieved effective inter-port interference management, which MIMO systems require through their notable isolation value of -28 dB at 2.4 GHz. The experimental results prove that fractal antenna designs meet the wireless system requirements by maintaining high operational efficiency along with precise polarization control and optimal impedance characteristics.

References

- [1] Vallappil A, Karimbu AK, Khawaja BA, Rahim MKA, Uzair M, Jamil M, Awais Q, "Minkowski–Sierpinski Fractal Structure-Inspired 2×2 Antenna Array for Use in Next-Generation Wireless Systems," *Fractal and Fractional*, vol. 7, no. 2, art. 158, 2023. <https://doi.org/10.3390/fractalfract7020158>.
- [2] Al Ka'bi A, "Design of a Microstrip Dual Band Fractal Antenna for Mobile Communications," *2022 IEEE International Black Sea Conference on Communications*

- and Networking, Sofia, Bulgaria, 2022, pp. 85-90. <https://doi.org/10.1109/BlackSeaCom54372.2022.9858198>.
- [3] Sediq T, Nourinia J, Ghobadi C, Mohammadi B, “A novel shaped ultrawideband fractal antenna for medical purposes,” *Biomedical Signal Processing and Control*, art. 104363, 2022. <https://doi.org/10.1016/j.bspc.2022.104363>.
- [4] Raj A, Mandal D, “Comparative analysis of fractal antennae for sub-6 GHz and 5G bands for wireless and IoT applications,” *Mobile Networks and Applications*, vol. 28, pp. 2258–2274, 2023. <https://doi.org/10.1007/s11036-024-02347-3>.
- [5] Ghadeer SH, Abd Rahim SK, Alibakhshikenari M, Virdee BS, Elwi TA, Iqbal A, Al Hasan M, “An innovative fractal monopole MIMO antenna for modern 5G applications,” *AEU - International Journal of Electronics and Communications*, art. 154480, 2022. <https://doi.org/10.1016/j.aeue.2022.154480>.
- [6] Benkhadda O, Saih M, Ahmad S, Abdullah Al-Gburi AJ, Zakaria Z, Chaji K, Reha A, “A Miniaturized Tri-Wideband Sierpinski Hexagonal- Shaped Fractal Antenna for Wireless Communication Applications,” *Fractal and Fractional*, vol. 7, no. 2, art. 115, 2023. <https://doi.org/10.3390/fractalfract7020115>.
- [7] Sran SS, Sivia JS, “Design of a Novel Wearable Hybrid Fractal Antenna for Wi-Fi, Bluetooth, and WiMax Applications,” *Wireless Personal Communications*, vol. 132, pp. 737–755, 2023. <https://doi.org/10.1007/s11277-023-10635-6>.
- [8] Palanisamy S et al., “A Novel Approach of Design and Analysis of a Hexagonal Fractal Antenna Array (HFAA) for Next-Generation Wireless Communication,” *Energies*, vol. 14, no. 19, art. 6204, 2021. <https://doi.org/10.3390/en14196204>.
- [9] Rahim A, Malik PK, “Analysis and design of fractal antenna for efficient communication network in vehicular model,” *Sustainable Computing: Informatics and Systems*, art. 100586, 2021. <https://doi.org/10.1016/j.suscom.2021.100586>.
- [10] Rahim A, Malik PK, Sankar Ponnappalli VA, “State of the Art: A Review on Vehicular Communications, Impact of 5G, Fractal Antennas for Future Communication,” *Proceedings of First International Conference on Computing, Communications, and Cyber-Security (IC4S 2019)*, Lecture Notes in Networks and Systems, vol 121, Springer, Singapore, 2020. https://doi.org/10.1007/978-981-15-3369-3_1.
- [11] Muthu Ramya, Rani R Boopathi, “A Compendious Review on Fractal Antenna Geometries in Wireless Communication,” 2020 International Conference on Inventive Computation Technologies (ICICT), Coimbatore, India, 2020, pp. 888-893. <https://doi.org/10.1109/ICICT48043.2020.9112580>.
- [12] Karmakar A, “Fractal antennas and arrays: a review and recent developments,” *International Journal of Microwave and Wireless Technologies*, vol. 13, no. 2, pp. 173-197, 2021. <https://doi.org/10.1017/S1759078720000963>.
- [13] Das S, Mitra D, Bhadra Chaudhuri SR, “Fractal loaded planar Super Wide Band four element MIMO antenna for THz applications,” *Nano Communication Networks*, art. 100374, 2021. <https://doi.org/10.1016/j.nancom.2021.100374>.
- [14] Sabaawi AMA, Sultan QH, Najm TA, “Design and Implementation of Multi-Band Fractal Slot Antennas for Energy Harvesting Applications,” *Periodica Polytechnica Electrical Engineering and Computer Science*, vol. 66, no. 3, pp. 253–264, 2022. <https://doi.org/10.3311/PPee>.

20301.

- [15] Kumar R, Sinha R, Choubey A, Mahto SK, “An ultrawide band monopole antenna using hexagonal-square shaped fractal geometry,” *Journal of Electromagnetic Waves and Applications*, vol. 35, no. 2, pp. 233–244, 2020. <https://doi.org/10.1080/09205071.2020.1829094>.
- [16] Paun M-A, Nichita M-V, Paun V-A, Paun V-P, “Minkowski’s Loop Fractal Antenna Dedicated to Sixth Generation (6G) Communication,” *Fractal and Fractional*, vol. 6, no. 7, art. 402, 2022. <https://doi.org/10.3390/fractalfract6070402>.